# Phenomenological description of neutron capture cross sections at 30 keV

**Miklós Kiss**

Berze N.J. Gimnázium, Kossuth 33, H-3200 Gyöngyös, Hungary
E-mail: kiss-m@chello.hu and

**Zoltán Trócsányi**

University of Debrecen and Institute of Nuclear Research of the Hungarian Academy of Sciences, H-4001 Debrecen P.O.Box 51, Hungary
E-mail: z.trocsanyi@atomki.hu



## Abstract

Studying published data of Maxwellian averaged neutron capture cross sections, we found simple phenomenological rules obeyed by the cross sections as a function of proton and neutron number. We use these rules to make predictions for cross sections of neutron capture on nuclei with proton number above 83, where very few data are available.

2011

# 1 Introduction

Theoretical descriptions of nucleosynthesis in stars rely heavily on the knowledge of capture cross sections of slow neutrons on nuclei. The classical model of nucleosynthesis in weak neutron flux is based on slow neutron capture (the $s$ process) that occurs along a path in the stability valley of nuclei (see for instance, Refs. [1–4]). The $s$-process evolution codes take into account the most important processes (those with largest cross sections) along the stability valley. The necessary information on the neutron capture cross sections and $\beta$ decay life times, needed to describe qualitatively the abundances of the $s$-process elements, is rather well known from laboratory experiments [5–8].

The $s$-process model is capable to explain the observed abundance of heavy elements fairly well [9]. The difference of observation and prediction is largely attributed to another process that occurs in stellar enviroment with high neutron flux, typically in supernovae. In such circumstances the neutron capture is very likely and neutron rich nuclei far from the stability valley build up very quickly due to repeated capture of neutrons. The nuclei produced such a way are so unstable and short-lived that experimental information about their capture cross sections and decay life times is not generally available.

In a recent work we proposed a unified model of nucleosynthesis of heavy elements in stars [10]. That approach takes into account all possible types of production and depletion mechanisms and solves the whole system of differential equations numerically. The result of such an approach is that (instead of the $s$-process path) the evolution of the synthesis proceeds along a band in the valley of stable nuclei. The width of this band – and consequently the final abundances of nuclei – depends on the neutron flux and the capture cross sections on individual nuclei charactherized by both their proton and neutron numbers, $\sigma(Z, N)$, which constitutes an essential input to the model calculations. Therefore, it is important to learn about these cross sections as much as possible.

In this paper, we study the general features of Maxwellian averaged neutron capture cross sections collected in recent compilations of data [7, 8]. In section 2 we show some phenomenological observations. In the following section we use those to make some order of magnitude predictions for the cature cross sections $\sigma(Z, N)$ for proton numbers $Z > 83$, where only very few data are available. Section 4 contains our conclusions.

# 2 Observations

Maxwellian averaged neutron capture cross sections (MACS) have been measured for many nuclei and made available in public data depositories. A comprehensive and complete review has been presented recently in Ref. [8]. Studying the available data, we can make

several observations: (i) although cross sections of many nuclei have been measured, there are still many missing, or rather uncertain data, especially for nuclei with $Z > 83$ (see Fig. 1a); (ii) the cross sections vary over very large range of values (about four orders of magnitude); (iii) for any fixed neutron number $N$ the the cross section is maximal for a corresponding value of the proton number $Z_{\rm max}$ and decreases rapidly as $|Z-Z_{\rm max}|$ increases (see Fig. 1b). The last point implies that in the $Z-N$ plain for each $N$ their is a unique value $Z_{\rm max}(N)$ where the capture cross section attains its maximal value. The existence of such a maximum is qualitatively easily understood: for fixed $N$, increasing $Z$ starting from a small value of $Z$, the capture of an additional $N$ stabilizes the nucleus in the strong repulsive Coulomb field of the protons, the binding energy per nucleon increases. However, for $Z$ above some value $Z_{\rm max}(N)$ the nucleus developes a neutron skin and additional neutrons become more and more loosely bound and capturing any further neutrons becomes less likely. The quantitavie understanding is certainly more complex, which however, is beyond the scope of the present paper.

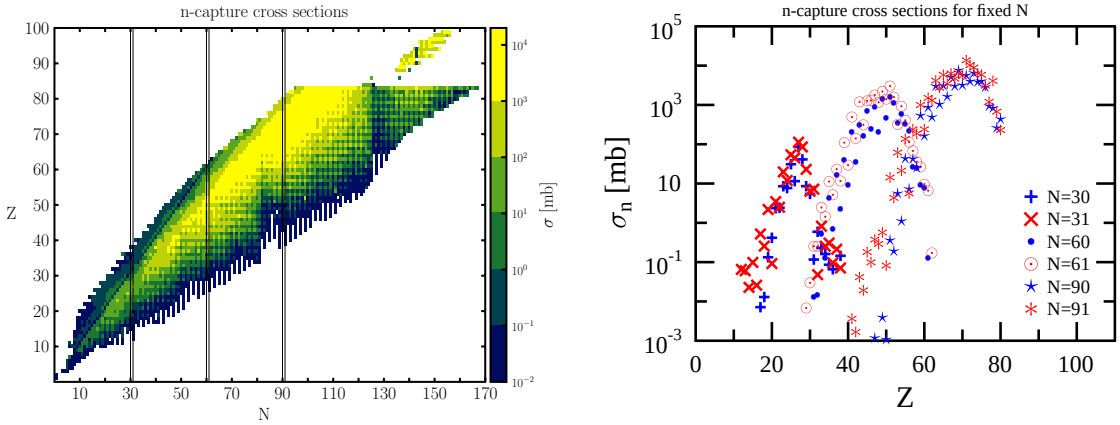


Figure 1: (a) MACS (at 30 keV) on nuclei as a function of the proton and neutron number. (b) Dependence on the proton number $Z$ of the MACS on nuclei with fixed neutron number $N = 30$, 31, 60, 61, 90 and 91 (indicated by vertical lines on Fig. 1a).

If we plot the $Z_{\rm max}(N)$ function then a rather simple picture emerges: it appears that a simple, almost linear function can describe the data, especially for small $N$. This feature becomes even more salient if we devide the nuclei into four groups according to the even/odd number of protons and neutrons: (i) $Z^{\rm (ee)}_{\rm max}$ for $Z$ even, $N$ even, (ii) $Z^{\rm (oo)}_{\rm max}$ for $Z$ odd, $N$ odd, (iii) $Z^{\rm (eo)}_{\rm max}$ for $Z$ even, $N$ odd, and (iv) $Z^{\rm (oe)}_{\rm max}$ for $Z$ odd, $N$ even, as shown in Fig. 2.

In Fig. 2 crosses mark the values of $Z_{\rm max}$ where the n-capture cross section is maximal for a fixed value of the neutron number $N$ as taken from Ref. [7]. The solid lines represent

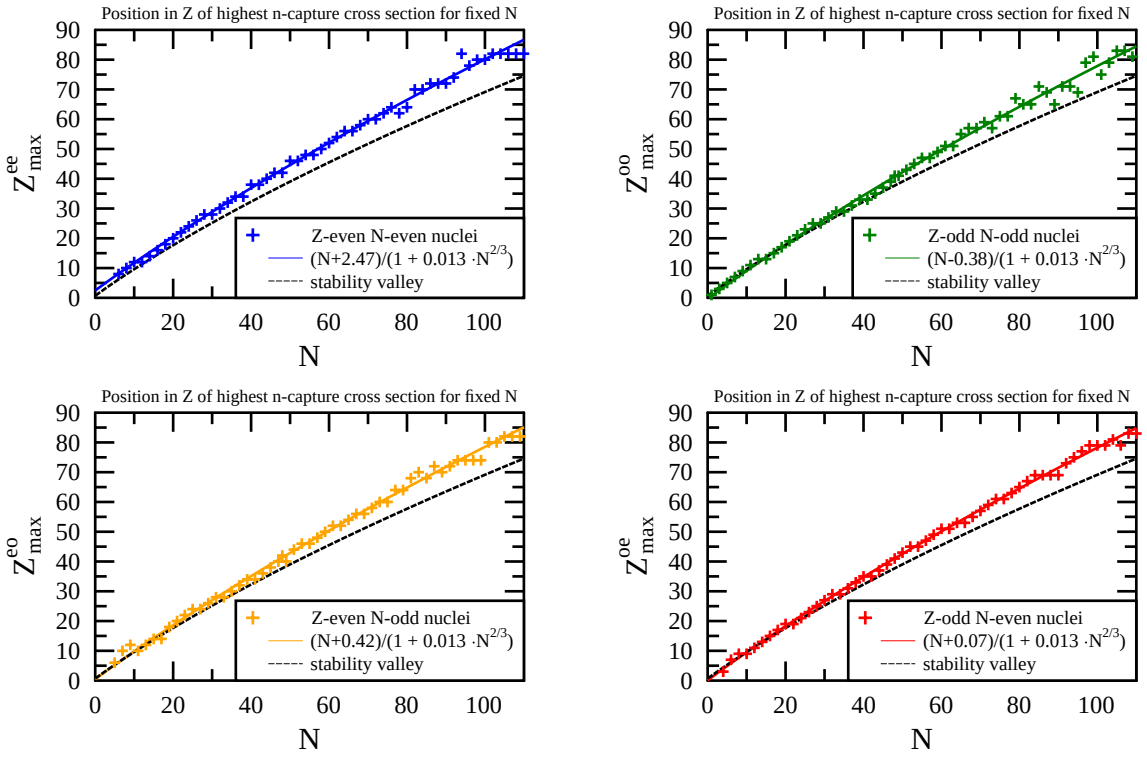


Figure 2: The function $Z_{\max}(N)$ for even-even, odd-odd, even-odd and odd-even nuclei. The crosses are the experimental values and the solid line represents the fit to the function in Eq. (1). The dashed line runs through the bottom of the stability valley.

fits of simple functions to these points in the form of

$$f(N; a_x, b, c) = \frac{N + a_x}{1 + bN^c}\,, \tag{1}$$

with $a_x$, $b$ and $c$ being fitted parameters, and $x$ = ee, oo, eo, or oe. We determined the values of these parameters in two steps. First, we minimized the function

$$\chi^2(a, b, c) = \sum_{i=1}^{214} \Big( Z_{\max}(N_i) - f(N; a, b, c) \Big)^2\,, \tag{2}$$

i.e. nuclei belonging to all four groups are taken into account and all points are assumed to have weight $\sigma_i = 1$. The upper limit in each group was chosen the largest value for which $Z_{\max}$ can be identified. With such a choice the we find $N^{(x)}_{\max} = 50$, 56, 53 and 55 maxima in the groups of even-even, odd-odd, even-odd and odd-even nuclei, respectively $(50 + 56 + 53 + 55 = 214)$. This fit gives

$$a = 0.060\,, \qquad b = 0.013\,, \qquad c = 0.666\,, \tag{3}$$

with correlation index

$$i = \sqrt{1 - \frac{\chi^2(a,b,c)}{\sum_{i=1}^{214}\Big(Z_{\max}(N_i) - \overline{Z}\Big)^2}} = \sqrt{1 - \frac{590.2}{116029}} = 0.997\,, \tag{4}$$

i.e. the coefficient of determination is almost one, $i^2 = 0.994$ ($\overline{Z} = \frac{1}{214}\sum_{i=1}^{214} Z_{\max}(N_i) = 45.5$).

In the second step we minimize the functions

$$\chi^2(a_x) = \sum_{i=1}^{N_{\max}^{(x)}} \Big(Z_{\max}^{(x)}(N_i) - f(N; a_x, 0.013, 0.666)\Big)^2 \tag{5}$$

separately for each group ($x$ = ee, oo, eo, oe). These fits result are

$$a_{\rm ee} = 2.47\,, \qquad a_{\rm oo} = -0.38\,, \qquad a_{\rm eo} = 0.07\,, \qquad a_{\rm oe} = 0.42\,, \tag{6}$$

with coefficient of determination above 0.99 in all cases.

We also exhibit the line of the stablity valley in Fig. 2, as a function of $N$ (instead of the usual $A = Z + N$)

$$Z_{\rm stab} = \frac{N + a_{\rm s}}{1 + b_{\rm s} N^{c_{\rm s}}}\,, \tag{7}$$

with parameters

$$a_{\rm s} = 0.682\,, \qquad b_{\rm s} = 0.027\,, \qquad c_{\rm s} = 0.614\,. \tag{8}$$

We see clearly that the highest n-capture cross sections lie above the stability valley and the separation grows with $N$.

We can also observe regularity in the Z-dependence of the cross section at fixed N (see Fig. 1b). We can extrapolate this regularity as well as the $Z_{\max}$ values to the region in the nuclide chart where very few data available for n-capture cross sections on nuclei (nuclei with proton number above 83, see Fig. 1a.

The first observation is a simple trend in the behaviour of the function $\sigma_{\max}(N) \equiv \sigma\Big(Z_{\max}(N)\Big)$. Putting $\sigma_{\max}(N)$ on a double logarithmic plot as shown in Fig. 3a (left panel), we find that the general trend is well described by a fourth-order power function,

$$\sigma_{\max}(N) = \left(\frac{N}{10}\right)^4 \text{ mb}\,. \tag{9}$$

This general trend is slightly modulated with some oscillatory behaviour, with minima around magic numbers, as seen on Fig. 3b, where the ratios of the measured cross sections to $\sigma_{\max}(N)$ are shown.

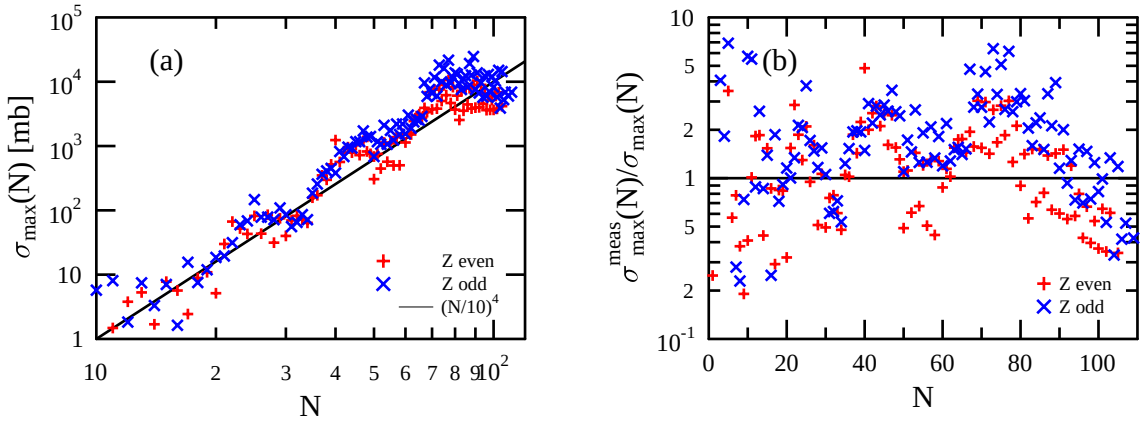


Figure 3: (a) Largest neutron capture cross sections as a function of the neutron number. (b) Ratio of the measured largest cross sections to $\sigma_{\max}$ given in Eq. (9).

The second observation is that if we normalize the cross sections $\sigma(Z,N)$ for a fixed neutron number $N$ with the largest cross section $\sigma_{\max}(N)$, then the profile of the dependence on the proton number is rather similar for all neutron numbers. This similarity is best seen if the position of the largest cross section is shifted by $-Z_{\max}$ to zero, therefore, we define these normalized and shifted cross section values,

$$\rho_N(z) = \frac{\sigma(z+Z_{\max},N)}{\sigma_{\max}(N)} \equiv \frac{\sigma(Z,N)}{\sigma\Big(Z_{\max}(N)\Big)}\,, \tag{10}$$

for all values of $N$, where data are available. Then we define the average by

$$\rho(z) = \frac{1}{N_z}\sum_{N=1}^{N_z}\rho_N(z)\,, \tag{11}$$

with squared standard deviation

$$\sigma(z)^2 = \frac{1}{N_z\,(N_z-1)}\sum_{N=1}^{N_z}\Big[\rho_N(z)-\rho(z)\Big]^2\,, \tag{12}$$

where $N_z$ is the number of available data for fixed $z$. This average is shown in Fig. 4. As seen from Fig. 4b this function is well approximated with an almost exponential function in both positive and negative directions, but with different exponents. More precisely, we fit the logarithm of the average with quadratic functions of the form $a_i z^2 + b_i z + c_i$ with subscript of the coefficients refering to three regions in $z$: (i) $i=1$ for $z<-26$, (ii) $i=2$ for $-26\le z<0$, and (iii) $i=3$ for $0<z$. For $i=2$ and 3 we fix $c_i=0$. This form ensures

Table 1: Result of the fit to the average function $\rho(z)$.

| $i$ | $a_i$ | $b_i$ | $c_i$ | $\chi^2$/d.o.f |
|---|---|---|---|---|
| 1 | 0.0044 | 1.135 | 17.95 | 5.29/5 |
| 2 | -0.0025 | 0.2658 | 0 | 6.15/9 |
| 3 | -0.0058 | -0.3948 | 0 | 7.14/4 |

the constraint $\rho(0) = 1$. We also require the continuity of the fitted function at $z = -26$. We measure the goodness of the fit by the weighted sum of squares

$$\chi^2 \simeq \sum_z \frac{\left[\ln \rho(z) - (a_i z^2 + b_i z + c_i)\right]^2}{\left(\frac{\sigma(z)}{\rho(z)}\right)^2}, \tag{13}$$

summed over values of $z$ in the three regions separately. The result of these fits is presented in Table 1 and shown in Fig. 4.

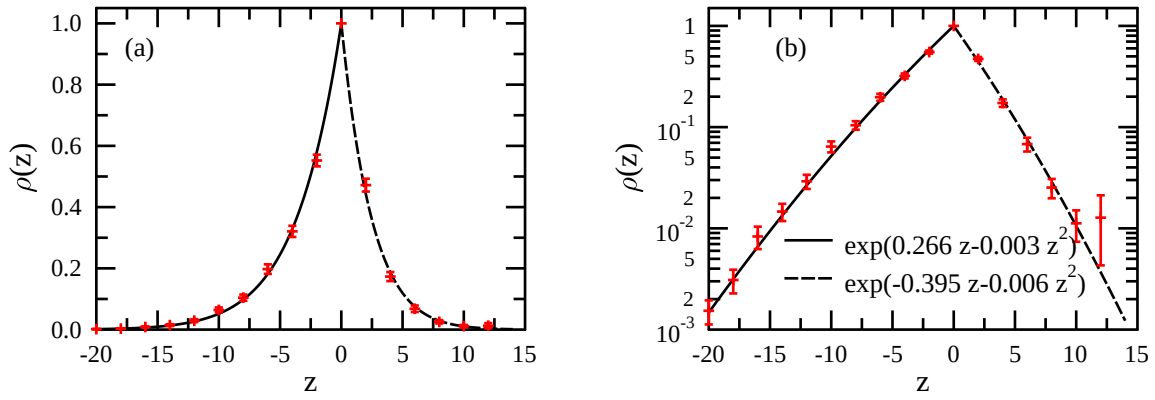


Figure 4: Average of the normalized neutron capture cross sections as a function of $z = Z - Z_{\max}$. The errorbars represent the standard deviation $\sigma(z)$.

Each function $\rho_N(z)$ differs from the average in two ways: (i) tipically the larger $N$ the wider $\rho_N(z)$ (as seen on Fig. 1a), (ii) in addition there are seemingly random fluctuations. The origin of the latter could be either a small physical effect, or simply error of the measurement: there are published values for cross sections $\sigma(Z, N)$ that differ by a factor of two. While it is difficult to consider the effect of the latter, the first effect can be taken into account by a simple appropiate scaling of the width of the average to those of the functions $\rho_N(z)$, which we discuss in the next section.

# 3 Predictions

The phenomenological observations made in the previous section can be used to make predictions for the order of magnitude of neutron capture cross sections in regions of the nuclide chart where experimental data are not available. We make these predictions in two steps. First we validate our procedure by comparing our predictions to measured cross sections. Then we use our procedure to make predictions.

## 3.1 Procedure

Our procedure relies on three pieces of information concluded from the analysis of the shape of *ridge of Maxwellian averaged neutron capture cross sections*:

1. position of $Z_{\rm max}$ as a function of the neutron number (location of the ridge top on the nuclide chart) obeys the simple function Eq. (1);
2. values of $\sigma_{\rm max}(N)$ (height of the ridge for given value of $Z_{\rm max}(N)$) obey the simple function Eq. (9);
3. characteristic behaviour of the average function $\rho(z)$ (slope of the ridge) is as given by Fig. 4.

In order to predict the cross section values for fixed neutron number, we proceed along the following steps:

1. Given $N$, find the position of $Z_{\rm max}$ from Eq. (1), which gives two maxima, one for even proton numbers ($Z^{\rm (e)}_{\rm max}$) and one for odd proton numbers ($Z^{\rm (o)}_{\rm max}$).
2. Given $Z_{\rm max}$ (either $Z^{\rm (e)}_{\rm max}$, or $Z^{\rm (o)}_{\rm max}$), position the maximum location of the average function $\rho(z)$ to $Z_{\rm max}$.
3. Scale the height and width of the function $\rho(z)$ to the available measured data by performing a two-parameter fit: (i) the scale factor of the height, (ii) the scale factor of the width.

The third step is hampered by the discrepancies in the measured cross section values, which can sometimes be quite significant as shown in Table 2 for heavy elements. Discrepancies exist among data for lighter elements, but generally within a factor of two [8].

Table 2: Ratios of largest and smallest measured neutron captured cross sections for elements beyond bismuth [8].

| nucleus | $\sigma_{\max}/\sigma_{\min}$ | nucleus | $\sigma_{\max}/\sigma_{\min}$ | nucleus | $\sigma_{\max}/\sigma_{\min}$ |
|---|---|---|---|---|---|
| $^{204}_{82}\mathrm{Pb}_{122}$ | 1.16 | $^{239}_{92}\mathrm{U}_{147}$ | 1.42 | $^{245}_{96}\mathrm{Cm}_{149}$ | 1.19 |
| $^{207}_{82}\mathrm{Pb}_{125}$ | 1.25 | $^{240}_{92}\mathrm{U}_{148}$ | 1.68 | $^{246}_{96}\mathrm{Cm}_{150}$ | 1.42 |
| $^{208}_{82}\mathrm{Pb}_{126}$ | 1.75 | $^{241}_{92}\mathrm{U}_{149}$ | 2.08 | $^{247}_{96}\mathrm{Cm}_{151}$ | 1.85 |
| $^{226}_{89}\mathrm{Ac}_{137}$ | 1.11 | $^{234}_{93}\mathrm{Np}_{141}$ | 3.05 | $^{250}_{96}\mathrm{Cm}_{154}$ | 1.42 |
| $^{227}_{89}\mathrm{Ac}_{138}$ | 15.9 | $^{235}_{93}\mathrm{Np}_{142}$ | 4.09 | $^{245}_{97}\mathrm{Bk}_{148}$ | 12.4 |
| $^{228}_{90}\mathrm{Th}_{138}$ | 1.75 | $^{236}_{93}\mathrm{Np}_{143}$ | 1.56 | $^{246}_{97}\mathrm{Bk}_{149}$ | 6.41 |
| $^{230}_{90}\mathrm{Th}_{140}$ | 3.32 | $^{238}_{93}\mathrm{Np}_{145}$ | 16.5 | $^{248}_{97}\mathrm{Bk}_{151}$ | 7.13 |
| $^{231}_{90}\mathrm{Th}_{141}$ | 16.7 | $^{239}_{93}\mathrm{Np}_{146}$ | 1.55 | $^{250}_{97}\mathrm{Bk}_{153}$ | 1.72 |
| $^{234}_{90}\mathrm{Th}_{144}$ | 2.43 | $^{236}_{94}\mathrm{Pu}_{142}$ | 3.08 | $^{248}_{98}\mathrm{Cf}_{150}$ | 3.45 |
| $^{229}_{91}\mathrm{Pa}_{138}$ | 4.97 | $^{237}_{94}\mathrm{Pu}_{143}$ | 1.96 | $^{250}_{98}\mathrm{Cf}_{152}$ | 1.82 |
| $^{230}_{91}\mathrm{Pa}_{139}$ | 1.77 | $^{238}_{94}\mathrm{Pu}_{144}$ | 1.39 | $^{251}_{98}\mathrm{Cf}_{153}$ | 1.34 |
| $^{231}_{91}\mathrm{Pa}_{140}$ | 2.14 | $^{243}_{94}\mathrm{Pu}_{149}$ | 1.44 | $^{252}_{98}\mathrm{Cf}_{154}$ | 2.96 |
| $^{232}_{91}\mathrm{Pa}_{141}$ | 2.82 | $^{246}_{94}\mathrm{Pu}_{152}$ | 12.3 | $^{253}_{98}\mathrm{Cf}_{155}$ | 20.0 |
| $^{233}_{91}\mathrm{Pa}_{142}$ | 1.90 | $^{240}_{95}\mathrm{Am}_{145}$ | 1.40 | $^{254}_{98}\mathrm{Cf}_{156}$ | 1.72 |
| $^{230}_{92}\mathrm{U}_{138}$ | 4.29 | $^{242}_{95}\mathrm{Am}_{147}$ | 22.7 | $^{251}_{99}\mathrm{Es}_{152}$ | 7.48 |
| $^{231}_{92}\mathrm{U}_{139}$ | 2.50 | $^{244}_{95}\mathrm{Am}_{149}$ | 1.34 | $^{252}_{99}\mathrm{Es}_{153}$ | 2.70 |
| $^{232}_{92}\mathrm{U}_{140}$ | 3.38 | $^{242}_{96}\mathrm{Cm}_{146}$ | 3.33 | $^{253}_{99}\mathrm{Es}_{154}$ | 46.8 |
| $^{233}_{92}\mathrm{U}_{141}$ | 1.40 | $^{243}_{96}\mathrm{Cm}_{147}$ | 2.03 | $^{254}_{99}\mathrm{Es}_{155}$ | 5.17 |
| $^{234}_{92}\mathrm{U}_{142}$ | 1.27 | $^{244}_{96}\mathrm{Cm}_{148}$ | 1.55 | $^{255}_{99}\mathrm{Es}_{156}$ | 3.19 |
| $^{237}_{92}\mathrm{U}_{145}$ | 1.89 | | | | |

## 3.2 Validation

We can compare the values of the predicted cross sections to those measured experimentally over the regions of the nuclide chart where data are abundantly available ($Z \leq 82$). In Fig. 5 we show again the cross sections of Fig. 1b together with the predicted values following from our procedure described in the previous subsection. Considering the simple nature of our procedure, the agreement between data and predictions is striking for all neutron numbers. Of course, the predictions rarely coincide exactly with the measurements, but the order of magnitude is usually correct, especially where the cross sections are large, which is the most important region for nucleosynthesis. Similar agreement can be observed over the large region of the nuclide chart where data are available.

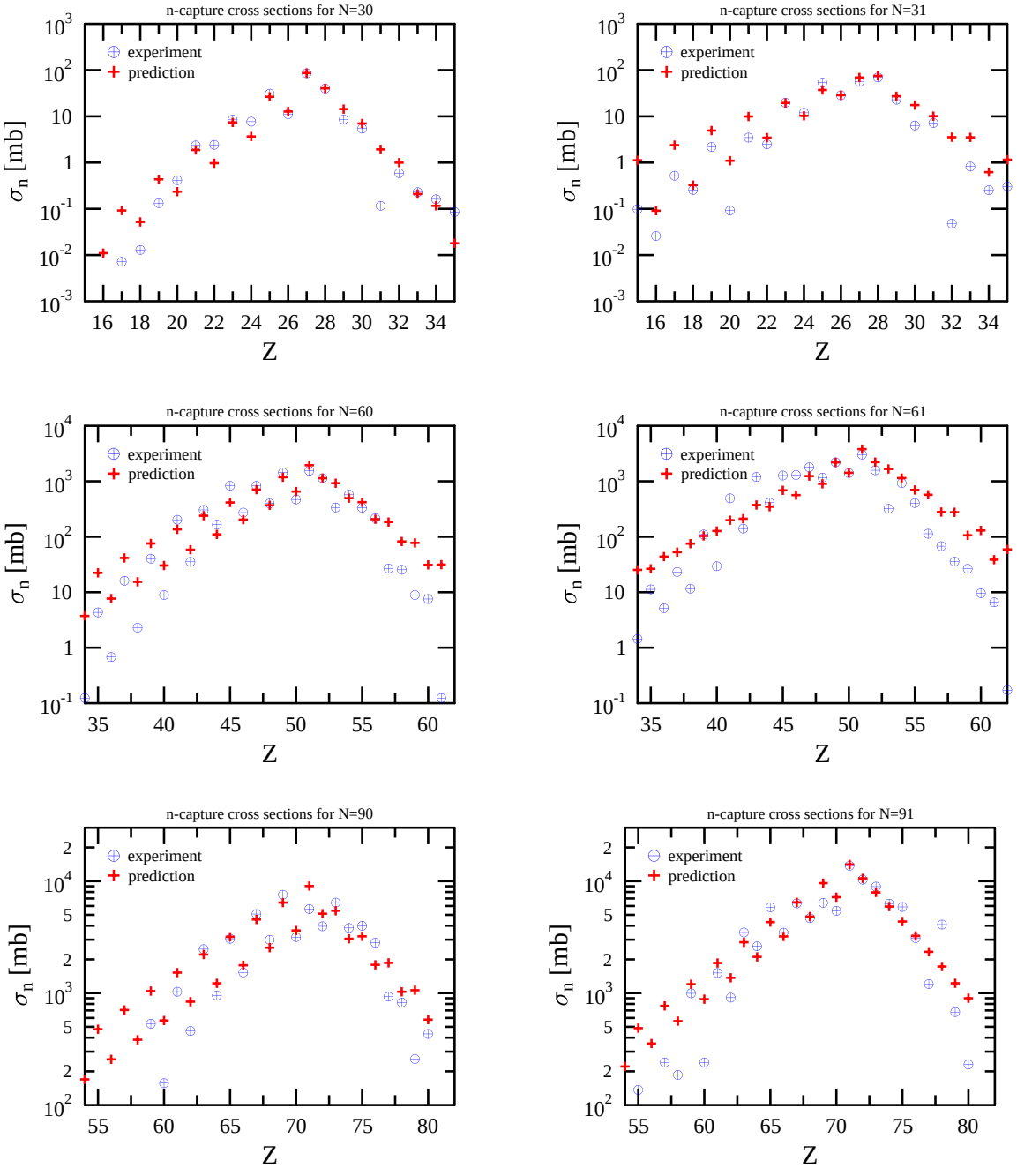


Figure 5: Dependence on the proton number $Z$ of MACS (at 30 keV) on nuclei with fixed neutron number $N = 30$, 31, 60, 61, 90 and 91: comparison of the predictions of the phenomenological model to measure data.

### 3.3 Predictions of unkown cross sections

Our procedure can be used to make prediction for cross sections in regions of the nuclide chart where *some* experimental information are available, such as $Z > 83$. In this region the general trend can be fitted to the measured data to complete the ridge. With such a procedure we obtain cross section values shown in Table 3. We can now use those preditions to complete the picture exhibited on Fig. 1. The result of such completion is shown in Fig. 6.

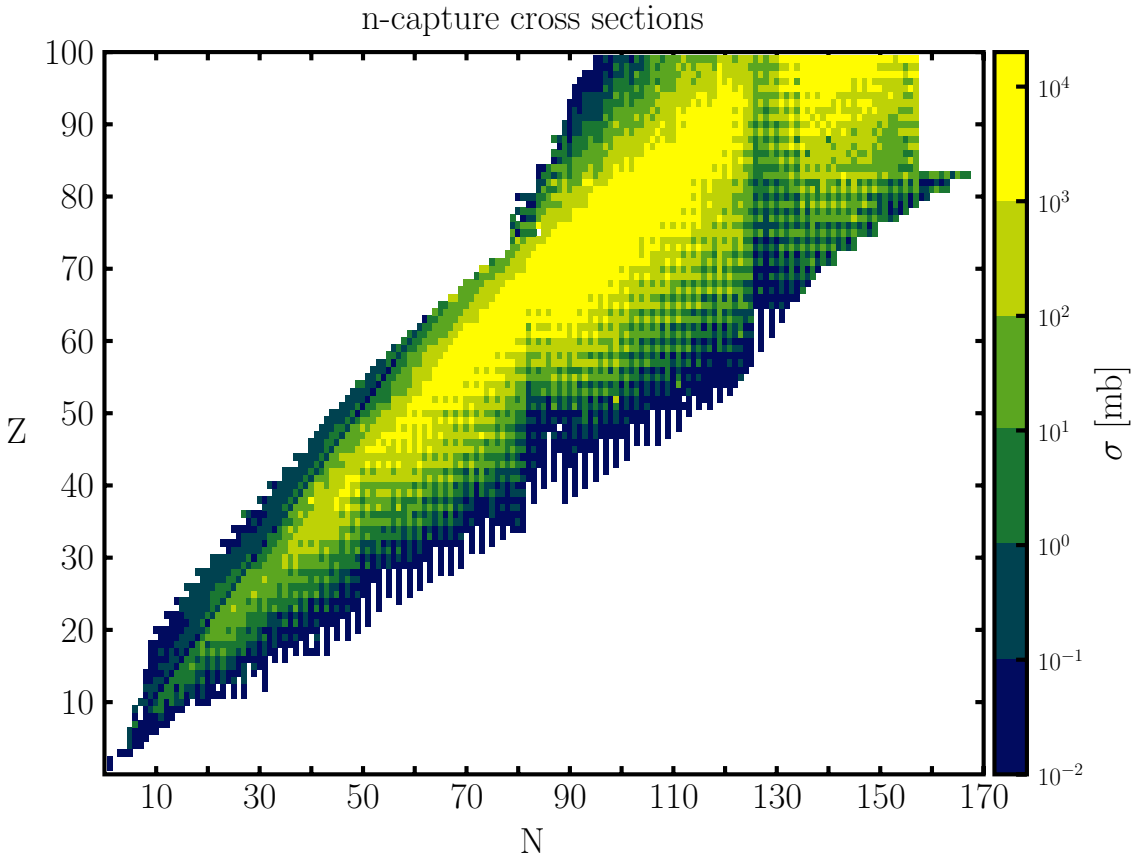


Figure 6: Ridge of MACS (at 30 keV) on nuclei as a function of the proton and neutron number.

## 4 Conclusions

We studied the dependence of the published MACS data on the proton and neutron number. We found a simple characteristic behaviour that we call the shape of the ridge of MACS in

Table 3: Predictions for neutron capture cross sections (in mbarns) as a function of the proton and neutron number for elements beyond bismuth.

| Z \ N | 132 | 133 | 134 | 135 | 136 | 137 | 138 | 139 | 140 | 141 | 142 |
|---|---|---|---|---|---|---|---|---|---|---|---|
| 84 | 3 | 28 | 3 | 216 | 53 | 331 | 99 | 121 | 90 | 157 | 82 |
| 85 | 74 | 577 | 99 | 772 | 534 | 229 | 530 | 171 | 385 | 29 | 215 |
| 86 | 6 | 59 | 5 | 330 | 3 | 512 | 156 | 205 | 150 | 259 | 146 |
| 87 | 135 | 1024 | 163 | 1276 | 875 | 437 | 792 | 302 | 693 | 74 | 376 |
| 88 | 13 | 118 | 8 | 601 | 227 | 653 | 448 | 343 | 6 | 421 | 258 |
| 89 | 242 | 1786 | 266 | 2083 | 1560 | 2020 | 1366 | 523 | 1229 | 184 | 650 |
| 90 | 26 | 233 | 15 | 751 | 252 | 1400 | 429 | 1400 | 433 | 1550 | 484 |
| 91 | 428 | 3063 | 428 | 3359 | 2269 | 600 | 1770 | 695 | 2140 | 1213 | 2250 |
| 92 | 51 | 450 | 25 | 1118 | 412 | 1790 | 427 | 492 | 770 | 425 | 1550 |
| 93 | 743 | 5168 | 681 | 5347 | 3590 | 2717 | 2514 | 1506 | 3692 | 600 | 1020 |
| 94 | 98 | 849 | 41 | 1648 | 666 | 2667 | 861 | 1496 | 1036 | 1693 | 750 |
| 95 | 1267 | 8577 | 1069 | 8406 | 5613 | 4816 | 3635 | 2499 | 6256 | 2345 | 3093 |
| 96 | 184 | 1568 | 68 | 2407 | 1063 | 3938 | 1289 | 2383 | 1631 | 2635 | 2191 |
| 97 | 2124 | 14000 | 1657 | 13048 | 8675 | 8379 | 5212 | 4087 | 10442 | 5132 | 5065 |
| 98 | 336 | 2831 | 111 | 3485 | 1675 | 5761 | 1913 | 3748 | 2538 | 4055 | 3611 |
| 99 | 3500 | 6718 | 2536 | 20000 | 13250 | 14312 | 7411 | 6584 | 17168 | 10876 | 8185 |
| 100 | 600 | 5000 | 178 | 5000 | 2605 | 8353 | 2813 | 5820 | 3904 | 6172 | 5873 |

the nuclide chart. This shape can be described by the position and height of the ridge and the decrease of the slope. Quantifying these characteristics, we made predictions for cross sections in regions of the nuclide chart where only few data are available. Such predictions are vital for computer programs aimed at simulating the formation of heavy elements in stars.

# Acknowledgments

This research was supported by the TÁMOP 4.2.1./B-09/1/KONV-2010-0007 project. We are grateful to I. Angeli for useful discussions.

# References


[1] M. E. Burbidge, G. R. Burbidge, W. A. Fowler and F. Hoyle, *Synthesis of the elements in stars*, Rev. Mod. Phys. **29**, 547 (1957).

[2] A. G. W. Cameron, *Nuclear astrophysics*, Ann. Rev. Nucl. Part. Sci. **8**, 299 (1958).

[3] F. Käppeler, H. Beer and K. Wisshak *s-process nucleosynthesis – nuclear physics and the classical model*, Rep. Prog. Phys. **52**, 945 (1989).

[4] R. Gallino *et al.*, *Evolution and Nucleosynthesis in Low-Mass Asymptotic Giant Branch Stars. II. Neutron Capture and the s-Process*, Astrophys. J. **497**, 388 (1998).

[5] Z. Y. Bao, H. Beer, F. Käppeler, H. Voss, K. Wisshak and R. Tauscher, *Neutron cross sections for nucleosinthesis studies*, Atomic Data and Nuclear Data Tables **76**, 70 (2000).

[6] I. Dillmann, M. Heil, F. Käppeler, R. Plag, T. Rauscher and F.-K. Thielemann, *KADoNiS - The Karlsruhe Astrophysical Database of Nucleosynthesis in Stars*, AIP Conf. Proc. 819, 123; online at http://www.kadonis.org

[7] T. Nakagawa, S. Chiba, T. Hayakawa, T. Kajino, *Maxwellian-averaged neutron-induced reaction cross sections and astrophysical reaction rates for kT = 1 keV to 1 MeV calculated from microscopic neutron cross section library JENDL-3.3*, Atom. Data Nucl. Data Tabl. **91**, 77 (2005). Available online 28 September 2005.

[8] B. Pritychenko, S. F. Mughaghab and A. A. Sonzogni, *Calculations of Maxwellian-averaged Cross Sections and Astrophysical Reaction Rates Using the ENDF/B-VII.0, JEFF-3.1, JENDL-3.3 and ENDF/B-VI.8 Evaluated Nuclear Reaction Data Libraries*, Atom. Data Nucl. Data Tabl. **96**, 645 (2010) [arXiv:0905.2086 [astro-ph.SR]]. Available on line at http://www.nndc.bnl.gov/astro/calcmacs.jsp

[9] C.E. Rolfs and W.S. Rodney, *Cauldrons in the Cosmos*, The University of. Chicago Press, (1988).

[10] M. Kiss and Z. Trócsányi, *A unified model for nucleosynthesis of heavy elements in stars*, J. Phys. Conf. Ser.: Nuclear Physics in Astrophysics IV, 012024 (2010).